Bone microstructure reconstruction From few projections with binary tomography

L.Wang, B.Sixou, F.Peyrin

CREATIS, Lyon, France

http://www.creatis.insa-lyon.fr

Outline

- **Background & Objective**
- **Binary Tomography**
- **Reconstruction methods**
  - TV
  - LS
  - PCLS
- **Results & Conclusions**

Background & Objective

- **Background**
  - Bone microstructure is important to diagnose osteoporosis
  - Requires high resolution CT and a high radiation dose

- **Discrete Tomography**
  - Reconstruct only a finite number of intensity levels (2 levels for binary image)
  - Limited number of views
  - Expected results: low noise, short scanning time

- **Objective**
  - Develop binary reconstruction methods from a limited number of projections for imaging 3D bone microstructure

State of Art

- **TV regularization**
  - Nonlinear total variation based noise removal algorithms *[L.I.Rudin, S.Osher, E.Fatemi, 1992]*
  - Solving constrained total variation image restoration and reconstruction problems via alternating direction methods *[MK.Ng, P.Weiss, X.Yuan,2010]*

- **Level-Set**
  - Nonlinear regularization for ill-posed problems with piecewise constant or strongly varying solutions *[A.Egger, L.Leitao, 2009]*
  - On multiple level-set regularization methods for inverse problems *[A.DeCezaro, A.Leitao, X.C.Ta, 2009]*
  - Bone microstructure reconstruction from few projections with level-set regularization *[B.Sixou, L.Wang, F.Peyrin, 2013]*

- **Piecewise Constant Level-Set**
  - On piecewise constant level-set (PCLS) methods for the identification of discontinuous parameters in ill-posed problems *[A.DeCezaro, A.Leitao, X.C.Tai, 2013]*

Problem Position

- **Binary Tomography**

$$Rf = p^{\delta} \quad s.t.\ f = (f_1, f_2, \cdots, f_n) \in \{0,1\}^n \tag{1}$$

Projection Operator | Discrete Image | Measured projection data | Binary constraints

- **Ill-posed problem: we estimate the discrete image f by minimization of regularization functional**

$$\hat{f} = argmin\, J(f) = argmin\, J_{data}(f) + \lambda J_{prior}(f) \tag{2}$$

Data Fidelity: $J_{data}(f) = \| Rf - p^{\delta} \|_{L_2}^2 \quad s.t. \| p - p^{\delta} \|_{L_2} < \delta$

noise level

Prior (TV, LS, etc.): $J_{prior}(f) \qquad Ex: \| Df \|_{L_2}^2$

Total Variation Regularization (TV)

- Optimization problem (P) :

$$(P)\ \ minimize\ \ \frac{\mu}{2} \parallel g - Rf \parallel + J_{TV}(f)\ \ s.t. f \in [0,1]^n \tag{3}$$

$$J_{TV}(f) = \sum_i \parallel D_i f \parallel_2^2$$ D_i - the discrete gradient operator at pixel i

- Minimization of the augmented Lagrangian by Alternate Direction Minimization Method (ADMM) *[M.Afonso, J.bioucas-Dias, M.Figeiredo, 2009]*

$$\hat{f} = \arg\min_f \mathcal{L}(f, (g_i), h, (\lambda_i)) = \frac{\mu}{2} \parallel g - Rf \parallel_2^2 + \sum_i [\parallel g_i \parallel_2 + \frac{\beta}{2} \parallel g_i - D_i f \parallel_2^2 - \lambda_i^t (g_i - D_i f)] + \frac{\beta}{2} \parallel h - f \parallel_2^2 \tag{4}$$

- ADMM with convex constraints

$$\hat{f} = \arg\min_f \mathcal{L}(f, (g_i), h, (\lambda_i), \lambda_C) = \frac{\mu}{2} \parallel g - Rf \parallel_2^2 + \sum_i \left[\parallel g_i \parallel + \frac{\beta}{2} \parallel g_i - D_i f \parallel_2^2 - \lambda_i^t (g_i - D_i f)\right] + I_C(h) + \frac{\beta}{2} \parallel h - f \parallel_2^2 - \lambda_C^t (h - f) \tag{5}$$

where μ is the regularization parameter and β is the Lagrangian parameter.

Total Variation Regularization (TV)

In this work, with the alternating minimization algorithm, the sequences $(f^k, g_i^k, h^k, \lambda_i^k, \lambda_C^k)$ are constructed with the following iterative scheme:

For each pixel i:

$$g_i^{k+1} = \max\{\| D_i f^k + \frac{1}{\beta}(\lambda_i^k) \|_2^2 - \frac{1}{\beta}, 0\} \frac{D_i f^k + \frac{1}{\beta}(\lambda_i^k)}{\| D_i f^k + \frac{1}{\beta}(\lambda_i^k) \|_2^2} \tag{6}$$

- The h^k update is:

$$h^{k+1} = \pi_C(f^k + \frac{\lambda_C^k}{\beta}) \tag{7}$$

where π_C is the projection of the convex set C.

- The f^k update is:

$$(\sum_i D_i^t D_i + \frac{\mu}{\beta} R^t R + I) f^{k+1} = \sum_i D_i^t (g_i^{k+1} - \frac{1}{\beta}\lambda_i^k) + \frac{\mu}{\beta} R^t g + h^{k+1} - \frac{\lambda_C^k}{\beta} \tag{8}$$

- The Lagrange multipliers (λ_i), λ_C are updated with:

$$\begin{aligned} \lambda_i^{k+1} &= \lambda_i^k - \beta\left(g_i^{k+1} - D_i f^{k+1}\right) \\ \lambda_C^{k+1} &= \lambda_C^k - \beta(h^{k+1} - f^{k+1}) \end{aligned} \tag{9}$$

Level-Set (LS)

- **Hypothesis:**
  - f: Piecewise constant, only two pixel values {0,1}

    It is the characteristic fct of a regular bounded set
  - θ is the level-set function

$$f = H(\theta) \; s.t. \; \theta \in H_1(\Omega)$$

where $H_1(\Omega)$ is the first order Sobolev Space, with:

$$H(\theta) = \begin{cases} 1 & if \; \theta > 0 \\ 0 & if \; \theta \leq 0 \end{cases}$$

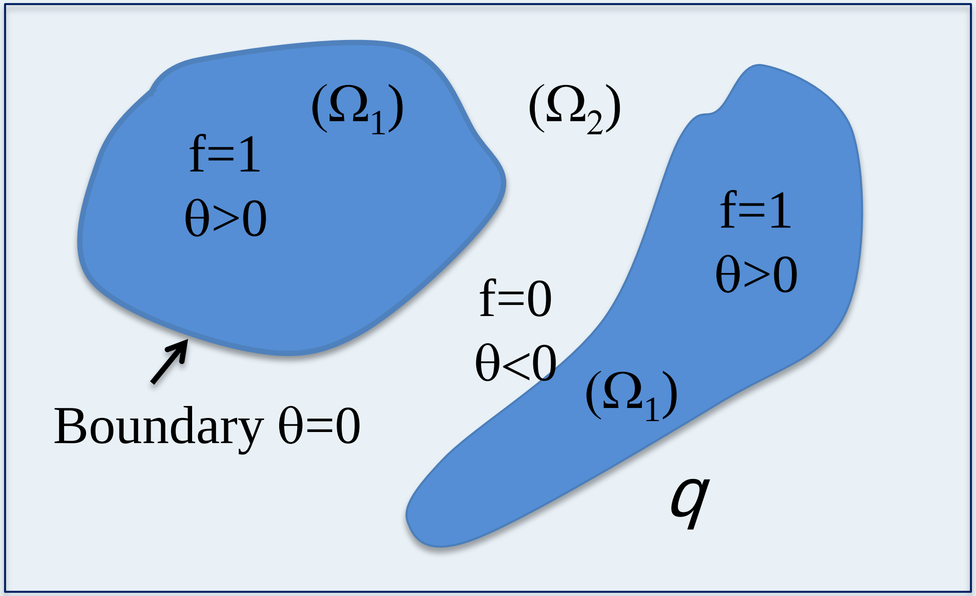

  - H is the Heaviside function
- Inverse problem theory for piecewise constant functions. *[Egger et al.(2009),De Cezaro et al.(2013)]*

Level-set (LS)

In the level-set regularization method, the function f in binary tomography is replaced with a Heaviside distribution $\theta \in H_1(\theta)$ and a level-set function θ:

- **Binary CT:** linear problem

  Find $f \in \{0,1\}^n$

  $$Rf = p^\delta$$

  Level-set: non-linear problem

  Find $\theta \in H_1(\Omega)$

  $$RH(\theta) = p^\delta$$

- **Variational approach**: minimize a level-set regularization functional

$$E(\theta) = \frac{\left\| RH(\theta) - p^\delta \right\|^2{}_2}{2} + \mathrm{F}(\theta) \qquad (10)$$

where $F(\theta)$ is the regularization term.

In our work, a T$V - H_1$ regularization function is considered:

$$F(\theta) = \beta_1 |H(\theta)|_{TV} + \beta_2 \|\theta\|_{H_1} \qquad (11)$$

where H_1 is the first order Sobolev space norm.

Level-Set (LS)

$$F(\theta) = \beta_1 \int |\nabla H(\theta)| dx + \beta_2 (\|\nabla\theta\|_{L_2}^2 + \|\theta\|_{L_2}^2) \quad (12)$$

The regularization parameters β_1, β_2 determine the relative weights of the stabilizing terms.

The first term $|H(\theta)|_{TV}$ is the Total Variation semi-norm, in the numerical implementation, it is necessary to replace the Heaviside function H by a smoothed approximation:

$$H_\varepsilon(x) = \frac{1+2\varepsilon}{\varepsilon}(er\,f(x/\varepsilon) + 1) - \varepsilon \quad (13)$$

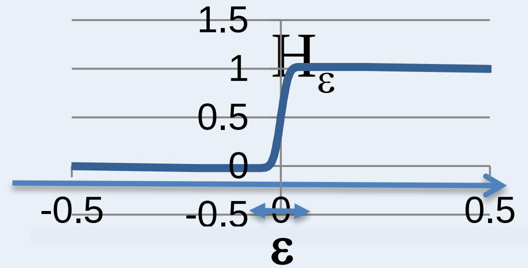

The minimizer of the regularization functional $E(\theta)$ can be approximated by the minimizer of a smoothed regularization functional $E_\varepsilon(\theta)$:

$$E_\varepsilon(\theta) = \frac{\left\|RH_\varepsilon(\theta) - p^\delta\right\|_2^2}{2} + \beta_1 |\nabla H_\varepsilon(\theta)|_{TV} + \beta_2 \|\theta\|_{H_1} \quad (14)$$

Piecewise Constant Level-Set (PCLS)

The function θ in binary tomography is replaced with a piecewise function f and the PCLS function *[A.DeCezaro et al, 2013]*:

Level-set :

Find $\theta \in H_1(\Omega)$

$\mathrm{RH}(\theta) = \mathrm{p}^\delta$

PC Level-set :

Find $f \in L_2(\Omega)$ s.t. $K(f) = f(f-1) = 0$

$Rf = p^\delta$

Minimization of the augmented Lagrangian:

$$\hat{f} = \arg min\ L(f,\lambda) = \arg min \frac{\|Rf - p^\delta\|_2^2}{2} + \beta \frac{\|K(f)\|^2{}_{L_2(\Omega)}}{2} + \int \lambda K(f) + \alpha |f|_{TV} \quad s.t. \alpha > 0 \qquad (15)$$

Given β, the solutions (f^*, λ^*) are obtained when $\frac{\partial L}{\partial f} = 0, \frac{\partial L}{\partial \lambda} = 0$.

- The gradient $\frac{\partial L}{\partial f}$ of the Lagrangian w.r.t f is given by:

$$R^*\left(Rf - p^\delta\right) + \beta K'^*(f)K(f) + \lambda K(f) + \alpha\ div\left(\frac{\nabla f}{|\nabla f|}\right) = 0 \qquad (16)$$

- The f^{k+1} update is:

$$f^{k+1} = f^k - \frac{\partial L}{\partial f} \qquad (17)$$

- The Lagrange multiplier λ update is:

$$\lambda^{k+1} = \lambda^k - K(f) \qquad (18)$$

Numerical Simulations

Data : experimental bone cross-section $(1024)^2$ acquired with synchrotron micro-CT, pixel size: 15 µm

Selection of a 256x256 ROI

Ground truth f^*: FBP reconstruction, 400 proj./ 400 rays per proj.

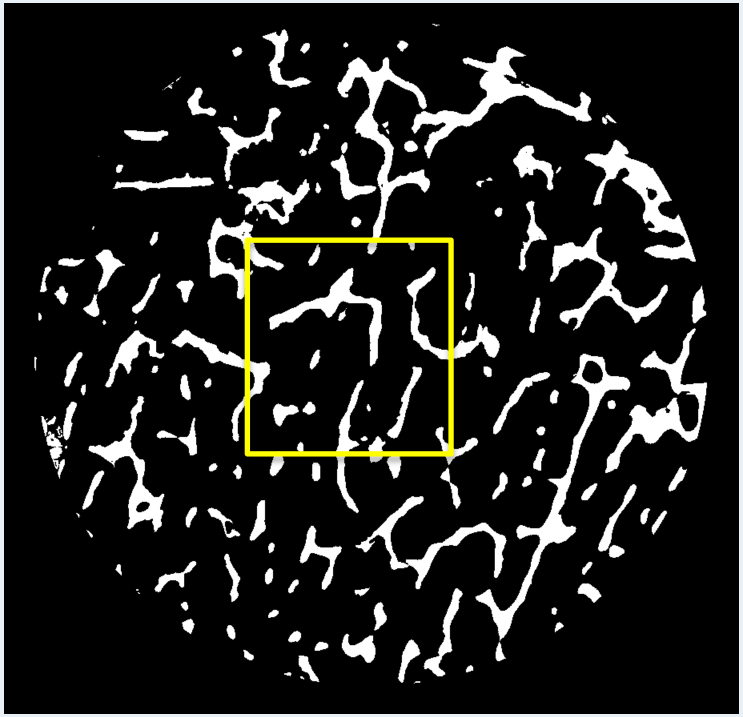

15mm

Numerical Simulations

(a) (b)

Fig.1 Ground-truth of disk image and Bone image

- Simulation details:
  - Additive gaussian noise with standard deviation: σ
  - Variable number of projection angles: M=20,50,100…
  - Morozov principle for choice of regularization parameter *[V.A.Morozov ,1984]*
  - Stopping criterion
  - Study of the evolution of the reconstruction errors
  - Quadratic Mean Square Error E_m and misclassification rate MR with σ
  - Difference maps

Reconstruction Images

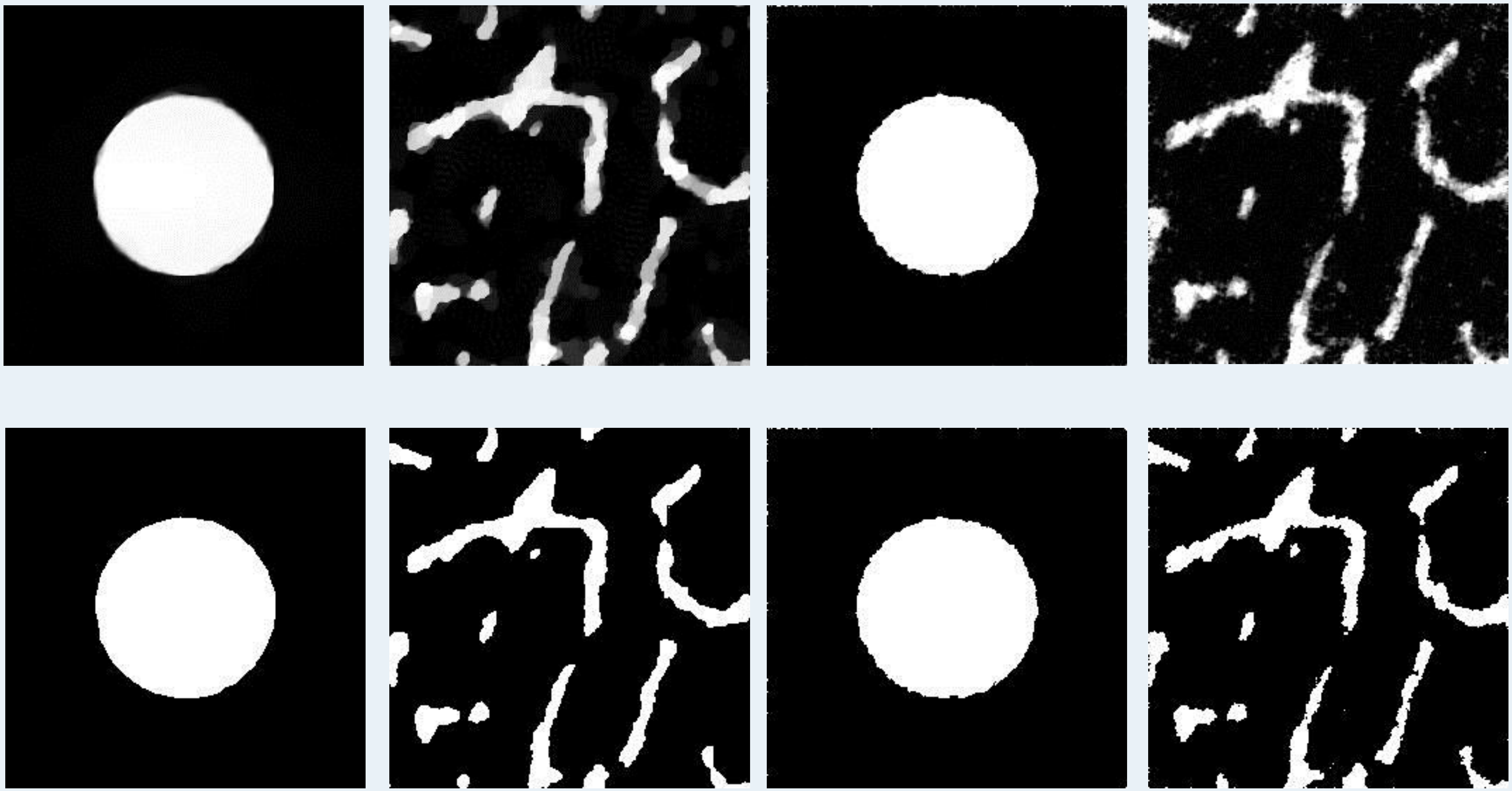

(a) TVbox-disk
$\sigma = 8.55$
$MR = 0.15\%$

(b) TVbox-bone
$\sigma = 6.57$
$MR = 1.79\%$

(c) LS-disk
$\sigma = 8.55$
$MR = 0.36\%$

(d) LS-bone
$\sigma = 6.57$
$MR = 2.39\%$

Fig. 2 Reconstruction images with projection angles $M = 20$, and 367 X-rays per projection.

Error Criterions

- The normalized mean square error E between ground-truth image f^* and reconstruction image f^k at iteration k is defined as:

$$E = \frac{\| f^k - f^* \|_2}{\| f^* \|_2} \tag{19}$$

$$E_m = \min_k E(k)\,, f^m = \arg\min_k E(k) \tag{20}$$

- The misclassification rate between the ground-truth image f^* and final binary image f_b is defined as:

$$MR = \frac{N_d}{N} \tag{21}$$

where N is the total number of pixels, N_d is the number of different pixels between binary image f_b and ground-truth image f^*. In our work, threshold is 0.5.

- The difference map image f_{diff} is defined as the difference between final binary image f_b and the ground-truth image f^*:

$$f_{diff} = |f_b - f^*| \tag{22}$$

- To obtain best reconstruction results, it is necessary to choose the optimal regularization parameters. Our choice is based on Morozov principle *[V.A.Morozov ,1984]*:

$$\| Rf^m(\mu) - p^\delta \| \approx \delta \tag{23}$$

where δ is the noise level, δ can be estimated as $\delta^2 = M \cdot N\sigma^2$. M is the number of projection angles, N is the number of X-ray per projection, μ is the regularization parameter, m is the iteration number.

- TV regularization

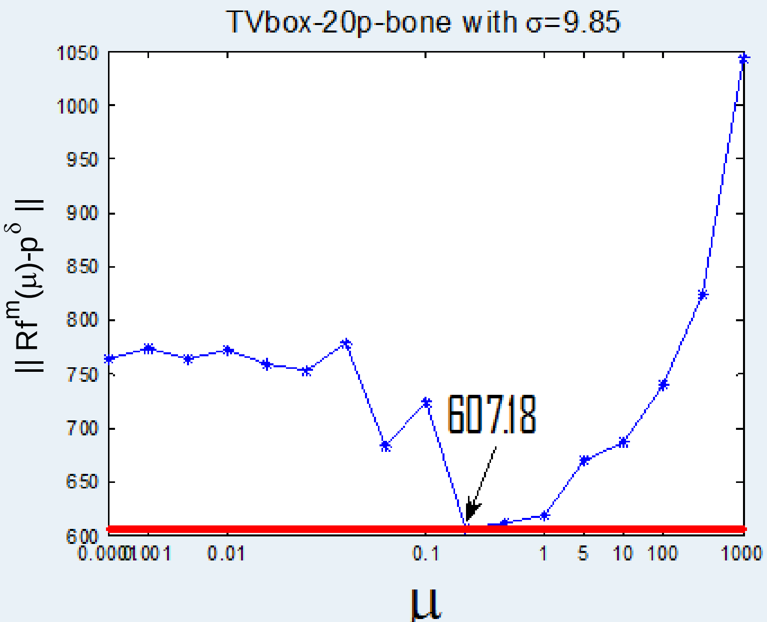

(a) $\| Rf^m(\mu) - p^\delta \|$

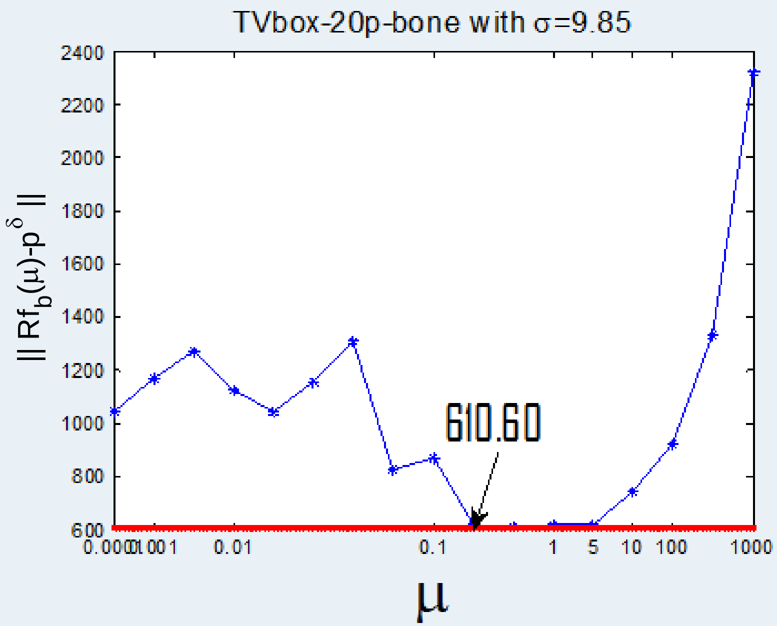

(b) $\| Rf_b(\mu) - p^\delta \|$

Fig.3 Noise level δ obtained with different μ

Stopping criterion

- It is necessary to stop the calculation at the best iteration m. Our choice is based on:

$$\frac{\| f^{k+1} - f^{k} \|}{\| f^{k} \|} < \epsilon \qquad (24)$$

where ϵ is a constant.

- TV regularization

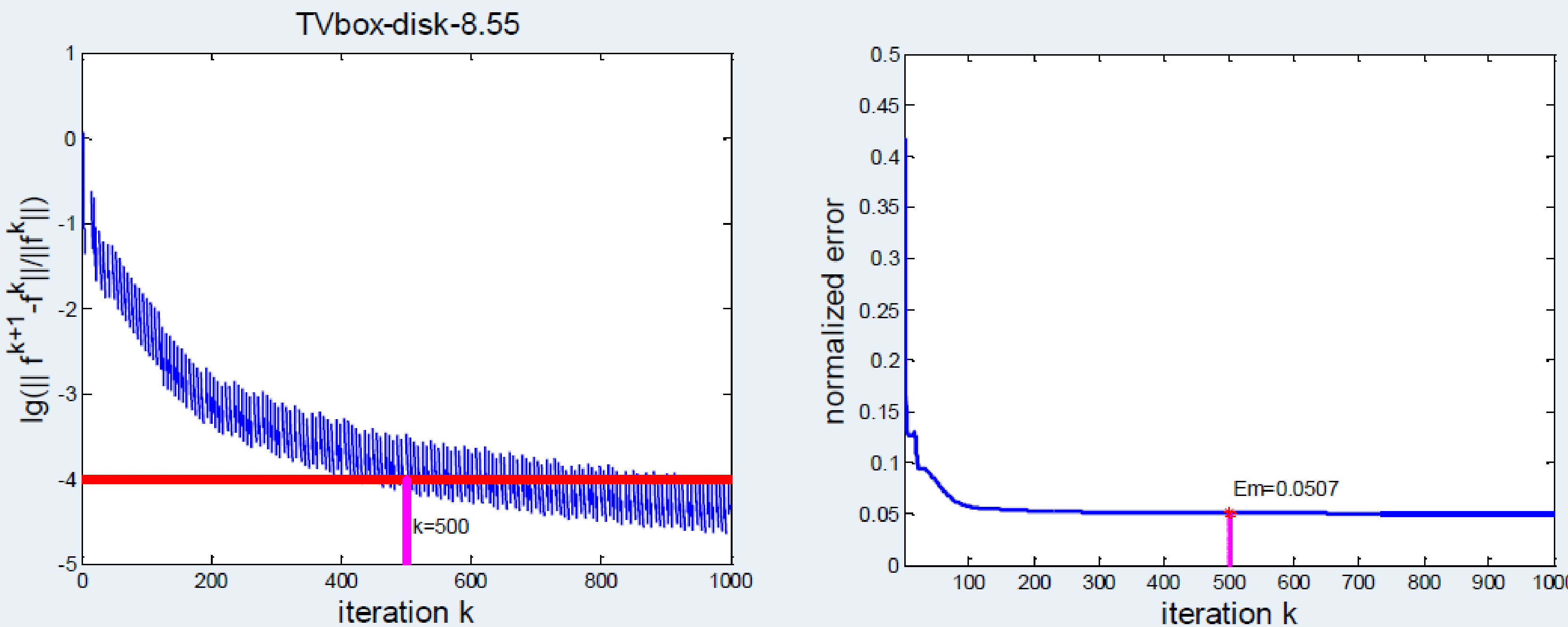

(a) $D_k = \lg(\frac{\|f^{k+1}-f^{k}\|}{\|f^{k}\|})$

(b) Error Evolution

Fig.4 (a) the evolution of $\lg(\frac{\|f^{k+1}-f^{k}\|}{\|f^{k}\|})$; (b) the evolution of normalized error.

Error evolution with iteration number

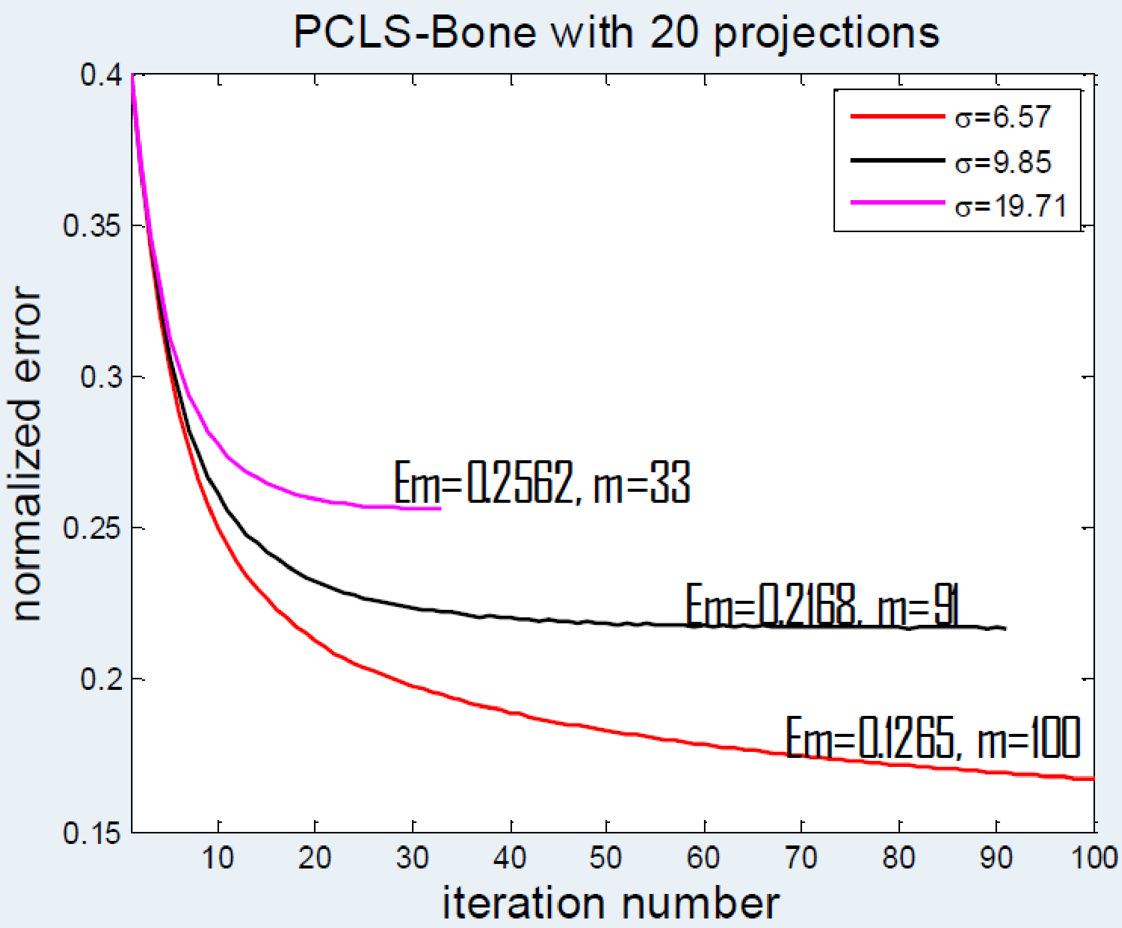

Fig.5 Error evolutions between gray-level reconstruction images and the ground-truth image

Quadratic Mean Square Error E_m with σ

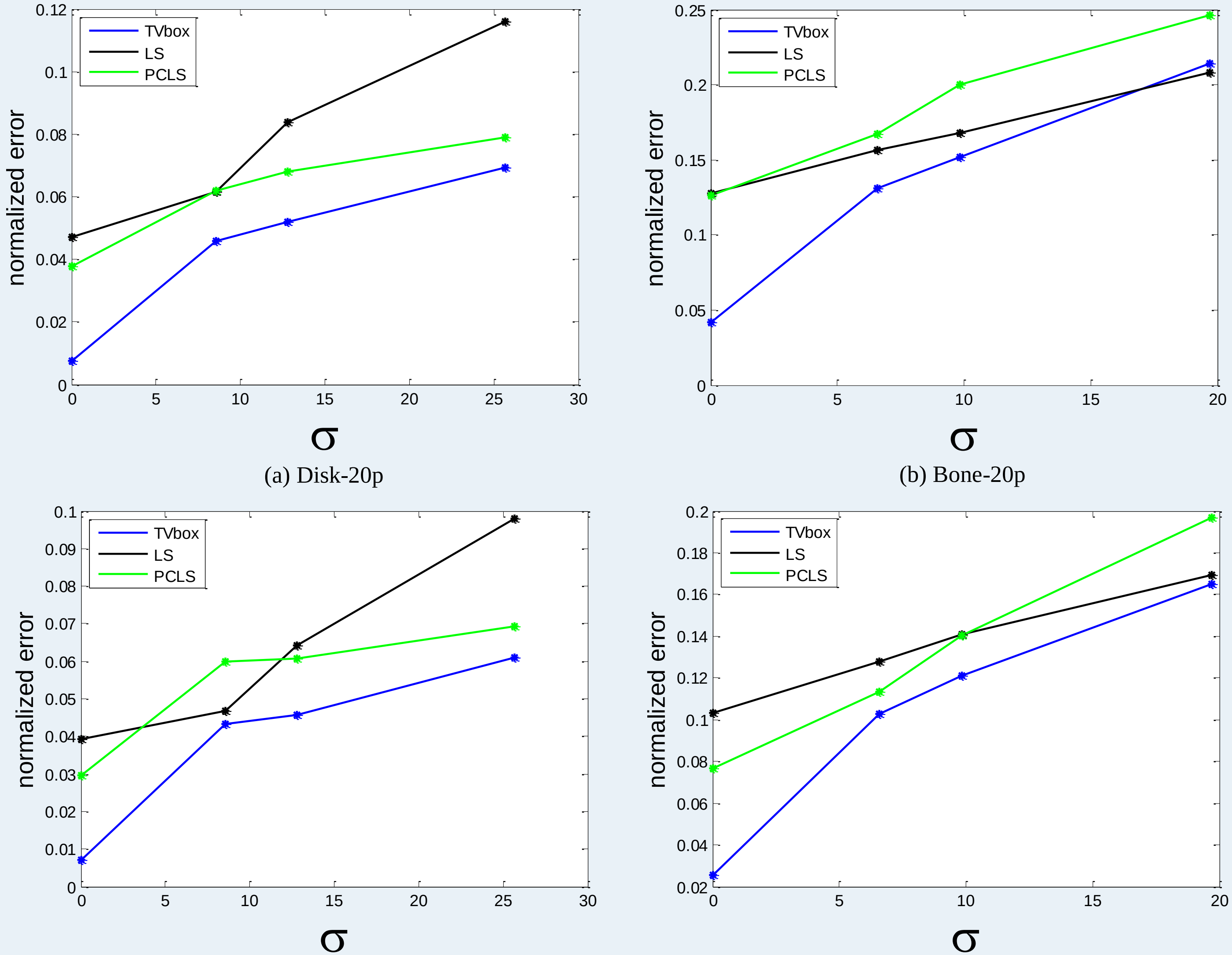

(a) Disk-20p (b) Bone-20p (c) Disk-50p (d) Bone-50p

Fig.6 The quadratic mean square errors with increase of σ

Misclassification Rates *MR* with σ

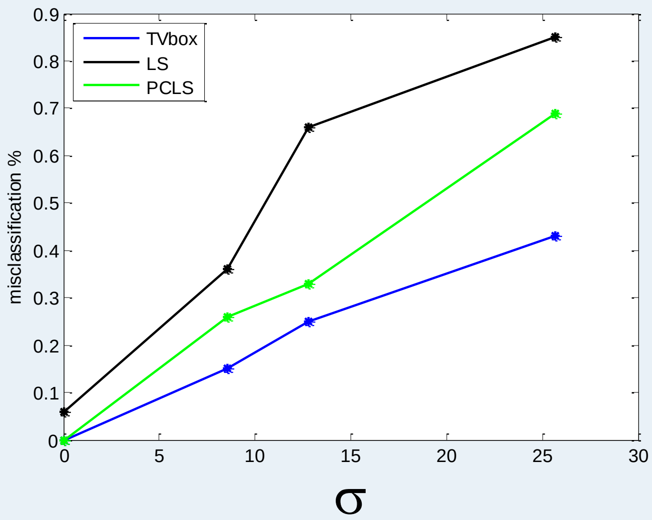

(a) Disk-20p

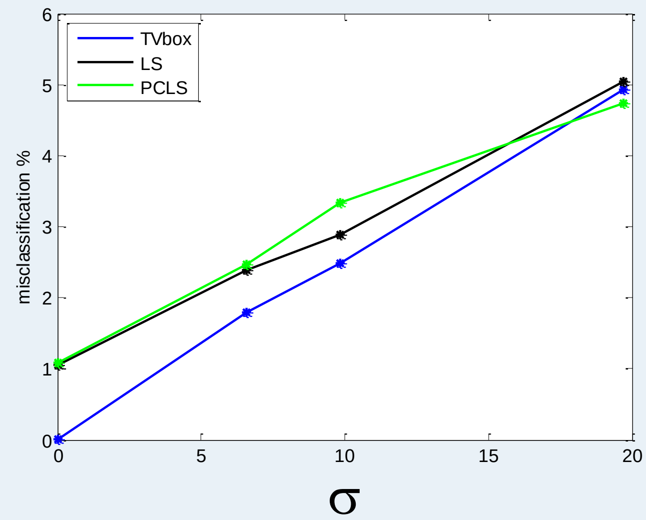

(b) Bone-20p

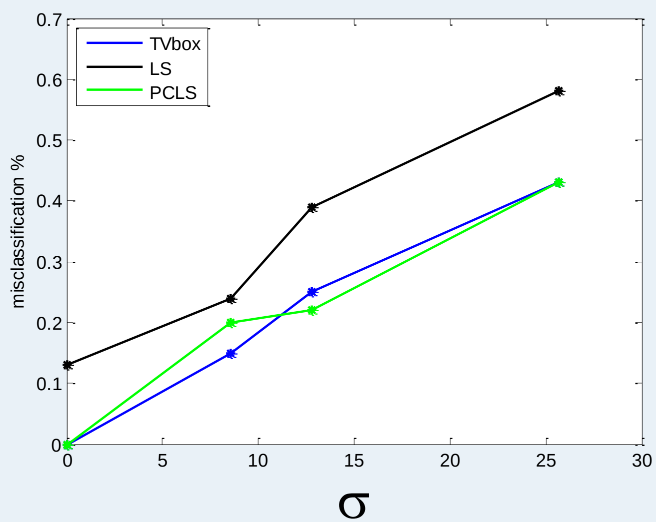

(c) Disk-50p

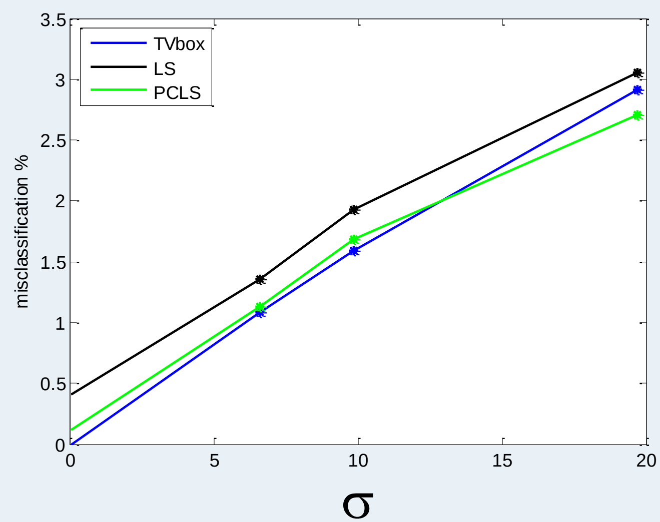

(d) Bone-50p

Fig.7 The misclassification rates with increase of σ

Difference Maps: TV

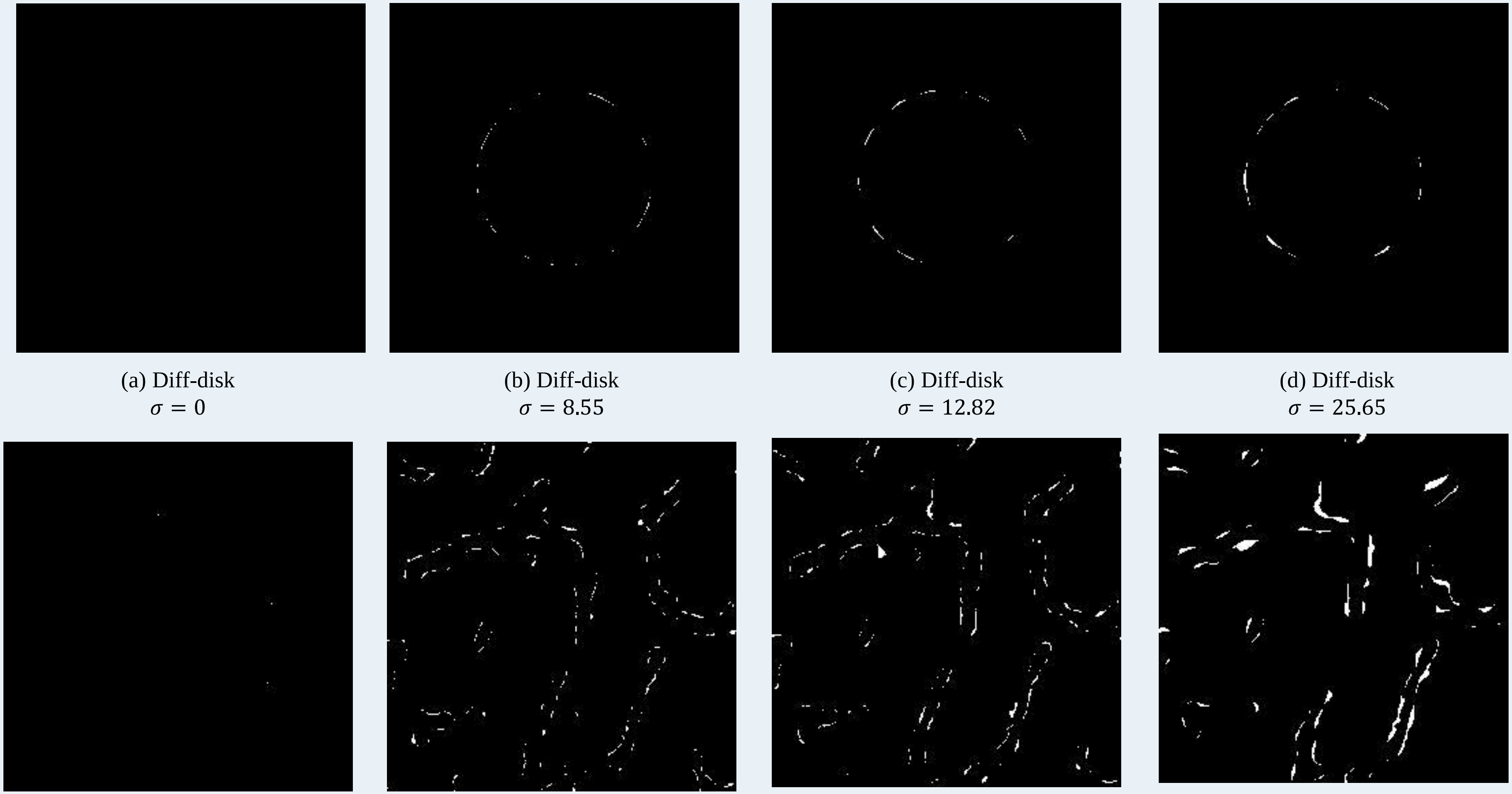

(a) Diff-disk $\sigma = 0$ (b) Diff-disk $\sigma = 8.55$ (c) Diff-disk $\sigma = 12.82$ (d) Diff-disk $\sigma = 25.65$

(e) Diff-bone $\sigma = 0$ (f) Diff-bone $\sigma = 6.57$ (g) Diff-bone $\sigma = 9.85$ (h) Diff-bone $\sigma = 19.71$

Fig.8 the difference maps of TV regularization with box constraints algorithm

Difference Maps: LS

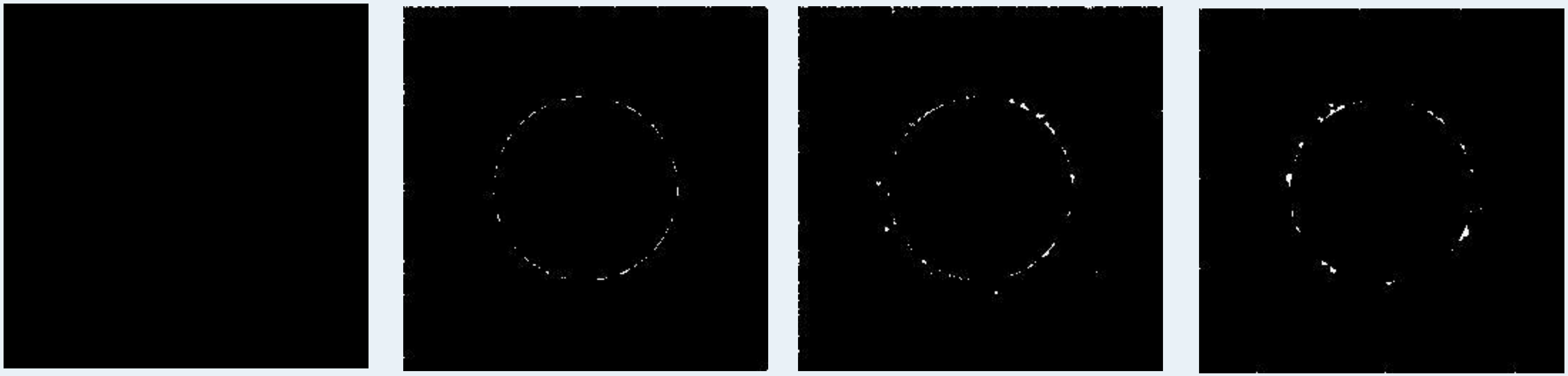

(a) Diff-disk $\sigma = 0$

(b) Diff-disk $\sigma = 8.55$

(c) Diff-disk $\sigma = 12.82$

(d) Diff-disk $\sigma = 25.65$

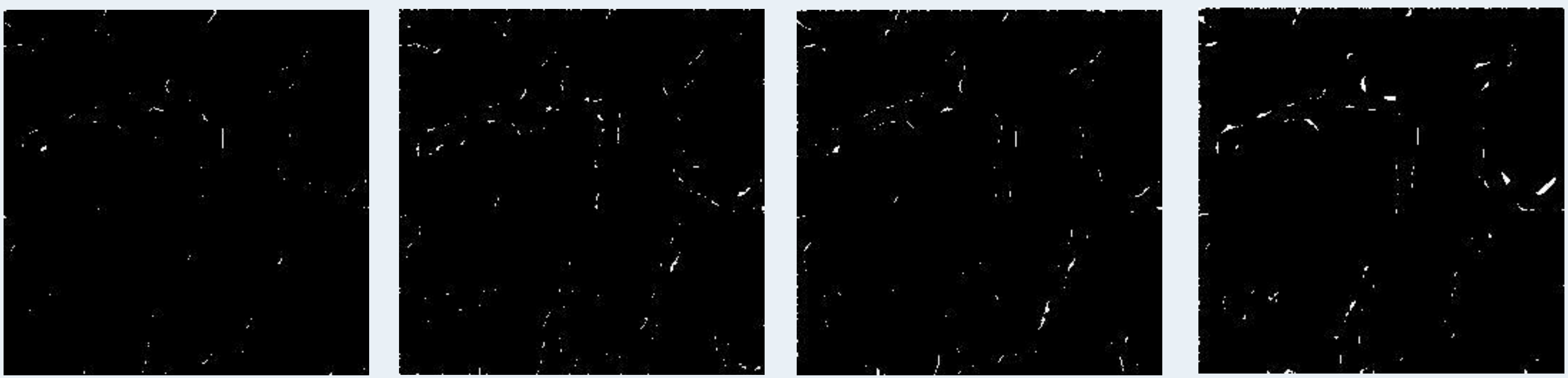

(e) Diff-bone $\sigma = 0$

(f) Diff-bone $\sigma = 6.57$

(g) Diff-bone $\sigma = 9.85$

(h) Diff-bone $\sigma = 19.71$

Fig.9 the difference maps of LS algorithm

Conclusions

Minimum errors:

- LS and PCLS algorithm convergent faster than TV regularization with box constraints.
- TV algorithm generated the best gray-level reconstruction results. Usually, PCLS performs better than LS on disk images, while worse on bone images.
- TV and PCLS give similar misclassification rates on binary images.

Misclassification rate:

- In my work, Threshold is set as 0.5. It gives the best binarization results.

Difference maps:

- From the difference maps of TV and LS, the reconstruction mistakes often occurs at boundary regions.
- With the increase of noise levels, the different regions between reconstruction image and ground-truth image become broader and broader.

Perspectives

- **Application to 3D bone microstructure data**
- **Investigate Stochastic Level-set algorithms**
- **Test multi-scale optimization methods**

Thanks very much!